Electronic Structure of Low-Spin Ferric Porphyrins: 13C NMR Studies of the Influence of Axial Ligand Orientation

ARTICLE *in* JOURNAL OF THE AMERICAN CHEMICAL SOCIETY · APRIL 1998

Impact Factor: 12.11 · DOI: 10.1021/ja983102m

Electronic Structure of Low-Spin Ferric Porphyrins: ^{13}C NMR Studies of the Influence of Axial Ligand Orientation

Ricardo O. Louro,[†] Ilidio J. Correia,[†] Lorraine Brennan,[‡] Isabel B. Coutinho,[†] Antonio V. Xavier,[†] and David L. Turner*[,‡]

Contribution from the Instituto de Tecnologia Química e Biológica, Universidade Nova de Lisboa, Oeiras, Portugal, and Department of Chemistry, University of Southampton, Southampton, United Kingdom

Received August 28, 1998

Abstract: Heteronuclear multiple quantum NMR is used to measure the paramagnetic ^{13}C shifts of the α substituents of the hemes in five different tetraheme ferricytochromes c_3. The shifts of the 20 bis-histidine ligated hemes are assigned and then analyzed in terms of a model based on the π molecular orbitals of the heme under perturbed D_4 symmetry, which yields the orientation of the rhombic perturbation, θ, and an energy splitting parameter, ΔE. Comparison of these parameters with crystal structures provides a test of the nature and extent of the influence of axial ligand orientation on the electronic structure of the heme. Despite possible differences between structures in solution and in the crystal, a clear correlation is found between θ and the resultant of the normals to the imidazole planes, and between ΔE and the angle between the normals. A weaker dependence of ΔE upon θ is also apparent. This is analogous to the results of low-temperature EPR studies of model compounds, which have been attributed to pseudo-Jahn−Teller distortion of the porphyrin. However, the effect is also predicted by extended Hückel calculations made with undistorted geometries. This work demonstrates that the variation in the electronic structure of bis-histidinyl hemes *c* is dominated by the geometry of the axial ligands and that other perturbations, such as asymmetric substitution of the porphyrin or low symmetry of the surrounding protein, are relatively minor. The correlations with θ and ΔE can, therefore, be used to determine the ligand geometry with sufficient accuracy to detect differences between structures in solution and in the crystal. The analysis can also be used to locate the principal axes of the magnetic susceptibility tensors of ferrihemes as well as providing orientational constraints for the axial ligands for the calculation of solution structures of paramagnetic proteins. This is particularly important since paramagnetic relaxation may make it impossible to observe NOE effects to the imidazole protons, leaving the geometry of the heme pocket poorly defined.

Introduction

The importance of the nature and geometry of axial ligands in influencing the properties of iron porphyrins is well-known. However, despite rapid early progress,[2−6] accurate separation of the effects of heme substitution, heme plane distortion, and the environment of the iron complex has proved surprisingly difficult. In particular, NMR studies of the electronic and magnetic properties of ferrihemes are complicated by the difficulty of ensuring that structural data are relevant to the sample conditions under which measurements are made. Crystallography is often the only source of atomic coordinates, but the structures in solution and in the crystal may be different, and ligands may be labile in solution. Such problems are conveniently minimized by using heme proteins as model compounds because the amino acid matrix stabilizes the heme geometry.

When a crystal structure is available, single-crystal EPR studies can be used to determine the magnetic susceptibility tensor with reasonable accuracy with respect to the structure, at least when there is a single paramagnetic center per unit cell.[7−9] However, the direct determination of the tensor by NMR studies of samples in solution requires extensive assignment of signals in a diamagnetic reference as well as in the paramagnetic complex.[3,10] The presence of paramagnetic metal centers in proteins dramatically alters their NMR spectra: the unpaired electrons induce contact and dipolar shifts in the resonances of nuclei near the paramagnetic center, so that the spectral

[†] Universidade Nova de Lisboa.

[‡] University of Southampton.

(1) Abbreviations used: EPR, electron paramagnetic resonance spectroscopy; NMR, nuclear magnetic resonance spectroscopy; NOE, nuclear Overhauser effect; NOESY, NOE spectroscopy; TOCSY, total correlation spectroscopy; DQF-COSY, double-quantum filtered correlation spectroscopy; HMQC, heteronuclear multiple quantum correlation; TRIS, tris-(hydroxymethyl)aminomethane; c3Dg, cytochrome c_3 from *Desulfovibrio gigas*; c3Dv, cytochrome c_3 from *Desulfovibrio vulgaris* (Hildenborough); c3Dd, cytochrome c_3 from *Desulfovibrio desulfuricans* ATCC 27774; c3Dn, cytochrome c_3 from *Desulfomicrobium norvegicum*; c3Db, cytochrome c_3 from *Desulfomicrobium baculatum* DSM 1743.

(2) Shulman, R. G.; Glarum, S. H.; Karplus, M. *J. Mol. Biol.* **1971**, *57*, 93−115.

(3) Keller, R. M.; Wüthrich, K. *Biochim. Biophys. Acta* **1972**, *285*, 326−336.

(4) La Mar, G. N.; Walker, F. A. *J. Am. Chem. Soc.* **1973**, *95*, 1782−1790.

(5) Traylor, T. G.; Berzinis, A. P. *J. Am. Chem. Soc.* **1980**, *102*, 2844−2846.

(6) Walker, F. A. *J. Am. Chem. Soc.* **1980**, *102*, 3254−3256.

(7) Horrocks, W.; Greenberg, E. S. *Biochim. Biophys. Acta* **1973**, *322*, 38−44.

(8) Byrn M. P.; Katz, B. A.; Keder, N. L.; Levan, K. R.; Magurany, C. J.; Miller, K. M.; Pritt, J. W.; Strouse, C. E. *J. Am. Chem. Soc.* **1983**, *105*, 4916−4922.

(9) Quinn, R.; Valentine, J. S.; Byrn, M. P.; Strouse, C. E. *J. Am. Chem. Soc.* **1987**, *109*, 3301−3308.

(10) Williams, G.; Clayden, N. J.; Moore, G. R.; Williams, R. J. P. *J. Mol. Biol.* **1985**, *183*, 447−460.

10.1021/ja983102m CCC: $15.00
Published on Web 12/04/1998

resolution may effectively be increased despite line broadening, but the patterns of proton chemical shifts which are typical for amino acid residues in diamagnetic proteins may be scrambled, making their assignment more difficult.[11,12] In principle, NMR data may be used to determine the structure of a complex directly in solution and hence avoid relying on crystal structures. Since the dipolar shifts are determined by a geometric function that depends on the position of the nucleus relative to the paramagnetic center and its magnetic axes,[13] they can be added to NOE-based distance constraints to improve the refinement of structures of paramagnetic proteins. Methods have been developed to fit structures to shifts calculated with a predetermined dipolar field,[14,15] or to optimize the structure together with the orientation of the magnetic axes with use of a program such as PSEUDYANA,[16] or to calculate the structure together with the complete magnetic susceptibility tensor, as demonstrated with the program PARADYANA.[17]

However, too few of the solution structures published to date are of sufficient quality for the empirical susceptibility tensors to be interpreted usefully in terms of the axial ligand orientations found in solution. Therefore, we chose to correlate NMR data with crystal structures, using a set of examples which is large enough to reveal any differences between the structures in the crystal and in solution. A more efficient and straightforward method than total assignment of diamagnetic and paramagnetic forms of each protein is then necessary for determining the magnetic and electronic properties of the large number of hemes to be used in the study.

If the magnetic *z* axis is assumed to be perpendicular to the heme plane, the orientation of the *x* and *y* axes can be obtained from dipolar shifts of nuclei of the heme and the anisotropy of the tensor may be extrapolated from low-temperature EPR *g*-values.[7] The essential difficulty with this approach is that delocalization of the unpaired electron induces substantial Fermi contact shifts, which must be separated from the dipolar contributions. Shulman et al.[2] proposed using the form of the heme molecular orbitals to calculate the Fermi contact contributions to the observed ^{1}H chemical shifts of heme protons, but this procedure is of limited accuracy because the hyperfine coupling constants are variable and the contact and dipolar contributions may be of similar magnitude.[18,19]

The dipolar shifts of ^{13}C nuclei in positions α to the tetrapyrrole ring are similar to those of their attached protons, but their Fermi contact shifts are very much larger.[20] For these nuclei, the shifts are dominated by the unpaired electron spin density at the neighboring β pyrrole carbon and so, far from attempting to make use of their dipolar shifts, the dipolar contribution to the paramagnetic shifts may be neglected completely.[21,22] Furthermore, spectra of heme proteins with natural abundance ^{13}C have become easily accessible through the development of specially designed pulse sequences and the increased sensitivity of the spectrometers.[23,24]

Thus, although ^{13}C shifts of the heme substituents are not useful for defining the dipolar field, they provide a direct insight into the form of the frontier molecular orbitals of the heme. In a six-coordinate ferriheme with D_{4h} symmetry, these form a degenerate pair of π orbitals which are dominated by the metal d_{xz} and d_{yz} atomic orbitals. The unpaired electron density on the β pyrrole carbons that determines the Fermi contact shifts of the α ^{13}C substituents is then a function of only two molecular orbital coefficients, labeled c_1 and c_5.[25] The reduced symmetry of hemes *c* within a protein mixes these orbitals and lifts the degeneracy, so the observed shifts are determined by two further parameters which describe the coupling and mixing between the orbitals.[2] We define an angular orbital mixing parameter, θ, as the angle between the orientation of the rhombic perturbation and the vector connecting the nitrogens of the pyrroles A and C of the heme:

$$|\Phi_x\rangle = \cos\theta\,|\phi_x\rangle + \sin\theta\,|\phi_y\rangle$$
$$|\Phi_y\rangle = \cos\theta\,|\phi_y\rangle - \sin\theta\,|\phi_x\rangle \qquad (1)$$

Also, an empirical energy splitting of the orbitals, ΔE, which determines the temperature dependence and asymmetry of the Fermi contact shifts, is defined with respect to a simple Boltzmann distribution of the unpaired electron in the two orbitals:[2,22,26]

$$\rho_i = \frac{c^2_{\Phi_x i} + \epsilon c^2_{\Phi_y i}}{1+\epsilon}; \quad \epsilon = \exp(-\Delta E/RT) \qquad (2)$$

These expressions are approximate for real heme complexes of low symmetry, but they provide a framework for analyzing experimental data that will reveal correlations only if the approximations are sufficiently good. Note also that ΔE should be zero in the absence of a rhombic perturbation although the Kramers doublets are split by the spin−orbit coupling. The parameter remains well-defined because the basis functions Φ_x and Φ_y have equal coefficients in the doublets of an axial system and, hence, equal spin density is associated with each of them.[26]

To test whether the orientation of the axial ligands is the dominant factor in controlling the heme electronic structure, the shifts of the ^{13}C resonances of the hemes in tetraheme cytochromes c_3 from five different species of sulfate-reducing bacteria were analyzed. The values determined for the orientation of the rhombic perturbation, θ, are compared with the orientation of bisector of the normals to the histidine planes, and the energy splitting of the orbitals, ΔE, is compared with the acute angle between the planes of the axial histidines available from the X-ray structures. The advantages in working with the tetraheme cytochromes c_3 are 3-fold. First, the hemes in these cytochromes have two histidines as axial ligands, and earlier work showed that both ligands make similar contributions to the calculated parameters.[22] Second, these are the only examples of small heme proteins with bis-histidinyl axial

(11) Bertini, I.; Luchinat, C. *NMR of Paramagnetic Molecules in Biological Systems*; Benjamin-Cummings: Menlo Park, CA, 1986.
(12) Xavier, A. V.; Turner, D. L.; Santos, H. *Methods Enzymol.* **1993**, *227*, 1−16.
(13) Barry, C. D.; North, A. C. T.; Glasel, A. J.; Williams, R. J. P.; Xavier, A. V. *Nature* **1971**, *232*, 236−245.
(14) Gochin, M.; Roder, H. *Protein Sci.* **1995**, *4*, 296−305.
(15) Guiles, R. D.; Sarma, S.; DiGate, R. J.; Banville, D.; Basus, V. J.; Kuntz, I. D.; Waskell, L. *Nature Struct. Biol.* **1996**, *3*, 333−339.
(16) Banci, L.; Bertini, I.; Bren, K. L.; Cremonini, M. A.; Gray, H. B.; Luchinat, C.; Turano, P. *J. Biol. Inorg. Chem.* **1996**, *1*, 117−126.
(17) Turner, D. L.; Brennan, L.; Chamberlin, S. G.; Louro, R. O.; Xavier, A. V. *Eur. J. Biophys.* **1998**, *27*, 367−375.
(18) La Mar, G. N.; Viscio, D. B.; Smith, K. M.; Caughey, M. L.; Smith, J. *J. Am. Chem. Soc.* **1978**, *100*, 8085−8092.
(19) Banci, L.; Bertini, I.; Pierattelli, R.; Vila, A. J. *Inorg. Chem.* **1994**, *33*, 4338−4343.
(20) Wüthrich, K.; Baumann, R. *Helv. Chim. Acta* **1974**, *57*, 336−350.
(21) Karplus, M.; Fraenkel, G. K. *J. Chem. Phys.* **1961**, *35*, 1312−1323.
(22) Turner, D. L.; Salgueiro, C. A.; Schenkels, P.; LeGall, J.; Xavier A. V. *Biophys. Biochim. Acta* **1995**, *1246*, 24−28.
(23) Müller, L. *J. Am. Chem. Soc.* **1979**, *101*, 4481−4484.
(24) Timkovich, R. *Inorg. Chem.* **1991**, *30*, 37−42.
(25) Longuet-Higgins, H. C.; Rector, C. W.; Platt, J. R. *J. Chem. Phys.* **1950**, *18*, 1174−1181.
(26) Turner, D. L. *Eur. J. Biochem.* **1995**, *227*, 829−837.

coordination for which there are crystal structures available. Third, they provide a dataset of 20 different hemes with a variety of orientations of the axial histidines, which provides a comprehensive test of the influence of the ligands. There is a slight complication in using multiheme proteins insofar as the nuclei in each heme are also subject to extrinsic dipolar shifts caused by other hemes, but these are even smaller than the intrinsic dipolar shifts so they may also be neglected.

In addition to testing the relationship between heme electronic structure and axial ligand geometry, these data provide estimates of the principal axes of the magnetic susceptibility tensors. If the *z* axis is perpendicular to the heme plane, the orientation of the rhombic perturbation is related to the orientation of the magnetic axes by counter-rotation,[8,26,27] so the value of θ obtained from ^{13}C contact shifts of the heme substituents can be used to fix the magnetic axes relative to the heme.[28] In fact, the major magnetic axis is found typically within a few degrees of the heme normal, and the tilt of the *z* axis in hemes with histidine and cyanide ligands has been associated with the orientation of the CN group.[29] Tilted *z* axes are also found in hemes with His-Met or bis-His ligation, and it has been noted that the *z* axis tends to lie in the plane of the imidazole.[30] Shokhirev and Walker[31] recently extended the analysis of the orientation of the in-plane axes to include all five iron d orbitals and concluded that linear counter-rotation of the rhombic perturbation and the magnetic axes appears to be a general rule for low-spin heme proteins.

With the magnetic axes placed relative to the heme, the anisotropy of the dipolar field can be extrapolated from the EPR *g*-values[7] and used to predict the dipolar shift for each nucleus. A preliminary test has been made for cytochrome c_3 from *D. vulgaris* (Hildenborough), in which the dipolar field defined by using the present model and the X-ray structure was shown to give a useful prediction of the dipolar chemical shifts of several residues and of the extrinsic dipolar effects of heme resonances.[32,33]

Materials and Methods

Cytochromes c_3 from *Desulfovibrio gigas* (c3Dg), *D. desulfuricans* ATCC 27774 (c3Dd), *Desulfomicrobium norvegicum* (formerly *D. desulfuricans* (Norway 4))[34] (c3Dn), and *Dsm. baculatum* DSM 1743 (c3Db) were purified as described in the literature.[35−37]

NMR samples were prepared by dissolving the lyophilized protein in ca. 500 μL of D_2O (99.96%) to a concentration of approximately 10 mM for c3Dg, 6 mM for c3Dd, 3.5 mM for c3Dn, and 1 mM for c3Db. The pH was adjusted with DCl or NaOD, and the values are reported without correction for the isotope effect.

The experiments with c3Dg were performed at pH 6.3 and 9.4, both at 298 and 307 K. For c3Dd, the spectra were obtained at pH 7.5 at 298 and 307 K. NMR spectra were acquired in a Bruker AMX500 spectrometer with a 5 mm inverse probe and a Eurotherm temperature controller. The NOESY experiments were performed with 10, 25, and 75 ms mixing times, and the TOCSY experiments with 42 ms spin-lock by using the MLEV17 sequence.[38] The water signal was suppressed by using a 200 ms selective pulse. The DQF-COSY spectra were obtained in phase-sensitive mode, with 500 ms presaturation for water suppression. The experiments with c3Dn and c3Db were performed in a Bruker DRX500 spectrometer, with a 5 mm inverse probe and a BVT3000 temperature controller. Spectra were obtained for c3Dn at 298 and 308 K at pH 5.0, and for c3Db at 293 and 303 K at pH 8.2. The NOESY experiments were performed with a 25 ms mixing time and the DQF-COSY spectra were obtained in phase-sensitive mode. The residual water signal was suppressed by application of a 1s presaturation pulse.

All $^1H-^{13}C$ HMQC spectra were obtained with use of natural abundance samples with ^{13}C decoupling during acquisition. The Δ delay was adjusted to optimize sensitivity according to the line widths of methyl signals.[39] The spectra were calibrated in the ^1H frequency by using TRIS as internal reference, with its pH-dependent shift calibrated separately against DSS, and in the ^{13}C frequency by using dioxane at 66.6 ppm.

The ^{13}C paramagnetic shifts of substituents α to the heme obtained at two temperatures were fitted to the model without correction for pseudocontact contributions. Because diamagnetic ^{13}C shifts have not been measured for these proteins, an average of the values available in the literature was used,[26] but the possible error in the reference shift is very much smaller than the paramagnetic shift in each case. The shifts of the substituents in all of the hemes were fitted simultaneously by using the Marquardt method, with separate values of ΔE and θ for each heme, together with a fixed value of the hyperfine coupling constant and optimized values for the two molecular orbital coefficients, c_1 and c_5, which applied to all hemes.

Results and Discussion

The assignment of the heme substituent resonances for c3Dg, c3Dd, c3Dn, and c3Db was performed as described previously for c3Dv:[22] the assignments of the proton and carbon signals for each protein in one set of experimental conditions are listed in Table 1. Table 2 reports the ^{13}C assignments of the α substituents of hemes for the cytochromes under the various experimental conditions used in this work. The few missing assignments correspond to signals with a small expected chemical shift, either in ^1H or in ^{13}C frequency, which could not be resolved from the protein envelope.

The ^{13}C chemical shifts of nuclei α to the hemes are plotted against those of the diametrically opposed substituents in Figure 1, showing the approximate symmetry of their paramagnetic shifts, which is an implicit requirement of the model. Only a small part of the asymmetry may be accounted for by extrinsic pseudocontact shifts induced by the other hemes present in each cytochrome, the remainder being attributable to the asymmetric substitution of the porphyrin, distortion of the macrocycle, or the low symmetry of the surrounding protein. The most extreme deviations arise from the thioether 3 and propionate 13 pairs from heme **3** (numbered according to the positions of the cysteinyl ligands in the cytochrome c_3 amino acid sequence) of c3Dd, c3Dn, and c3Db, which might be a consequence of the close proximity of a lysine side chain (lysine 38 in c3Dn and c3Db and lysine 90 in c3Dd) to the propionate. However, the fitted parameters are virtually unaffected by excluding these

(27) Oosterhuis, W. T.; Lang, G. *Phys. Rev.* **1969**, *178*, 439−456.
(28) Pierattelli, R.; Banci, L.; Turner, D. L. *J. Biol. Inorg. Chem.* **1995**, *1*, 320−329.
(29) La Mar, G. N.; Chen, Z.; Vyas, K.; McPherson, A. D. *J. Am. Chem. Soc.* **1995**, *117*, 411−419.
(30) Brennan, L.; Turner, D. L. *Biochim. Biophys. Acta* **1997**, *1342*, 1−12.
(31) Shokhirev, N. V.; Walker, F. A. *J. Am. Chem. Soc.* **1998**, *120*, 981−990.
(32) Salgueiro, C. A.; Turner, D. L.; Xavier A. V. *Eur. J. Biochem.* **1997**, *244*, 721−734.
(33) Salgueiro, C. A.; Turner, D. L.; LeGall, J.; Xavier, A. V. *J. Biol. Inorg. Chem.* **1997**, *2*, 343−349.
(34) Genthner, B. R. S.; Friedman, S. D.; Devereux, R. *Int. J. Syst. Bacteriol.* **1997**, *47*, 889−892.
(35) Liu, M. C.; Costa, C.; Coutinho, I.; Moura, J. J. G.; Moura, I.; Xavier, A. V.; LeGall, J. *J. Bacteriol.* **1988**, *170*, 5545−5551.
(36) Coutinho, I. B.; Xavier, A. V. *Methods Enzymol.* **1994**, *243*, 119−140.
(37) Louro, R. O.; Catarino, T.; Turner, D. L.; Piçarra-Pereira, M. A.; Pacheco, I.; LeGall, J.; Xavier, A. V. *Biochemistry* **1998**, *37*, 15808−15815.
(38) Bax, A.; Davies, D. G. *J. Magn. Reson.* **1985**, *63*, 355−360.
(39) Louro, R. O.; Medina, M.; Aguiar, A. P.; Hervás, M.; De la Rosa, M.; Gómez-Moreno, C.; Turner, D. L.; Xavier A. V. *J. Biol. Inorg. Chem.* **1998**, *3*, 68−73.

Table 1. Chemical Shifts (ppm) of Heme Resonances[a]

	heme **1**		heme **2**		heme **3**		heme **4**	
	^{13}C	^{1}H	^{13}C	^{1}H	^{13}C	^{1}H	^{13}C	^{1}H
A. Assignment of Heme Resonances for c3Dd at pH 7.6 and 298 K								
M2^{1}	−50.8	22.86	−24.2	4.02	−34.4	14.30	−49.2	21.90
H3^{1}	n.d.	n.d.	n.d.	n.d.	−29.8	−1.38	n.d.	n.d.
H3^{2}	n.d.	n.d.	n.d.	n.d.	74.1	−2.75	n.d.	n.d.
M7^{1}	−5.4	4.65	−42.3	23.30	−28.8	10.40	−7.0	6.90
H8^{1}	−36.5	−4.35	−29.7	2.18	n.d.	n.d.	−35.2	0.86
H8^{2}	72.6*	−3.49	85.7*	2.13*	n.d.	n.d.	n.d.	2.36*
M12^{1}	−57.3	19.47	−22.8	6.03	−41.5	23.49	−46.4	16.60
P13^{1}	7.7	1.25	−12.0	3.29	−61.2	25.54	11.0	−0.41
		−3.08		0.31		15.27		−3.44
P17^{1}	0.1	5.00	−30.0	15.79	n.d.	n.d.	13.7*	2.32*
		1.78		4.83*				0.93*
M18^{1}	−60.4	27.81	−48.5	23.26	0.3	−3.27	−58.7	28.32
B. Assignment of Heme Resonances for c3Dg at pH 6.3 and 298 K								
M2^{1}	−41.4	16.97	−24.4	4.86	−34.5	14.45	−45.0	19.39
H3^{1}	n.d.	−0.68*	n.d.	−0.58	−32.0	0.25	22.4*	1.70*
H3^{2}	n.d.	−1.84 *	19.3	−3.64	70.5	−2.15	17.7*	−0.22*
M7^{1}	−16.4	11.64	−38.4	23.58	−28.5	9.56	−12.0	9.74
H8^{1}	−42.8	−2.94	−34.8	2.05	n.d.	−0.38*	−35.7	1.58
H8^{2}	47.5	−0.36	92.8	2.68	n.d.	−0.93*	56.9*	2.90*
M12^{1}	−48.3	14.91	−28.0	7.96	−39.4	21.62	−40.0	13.82
P13^{1}	10.5	−1.06	3.8	−0.94	−55.2	17.95	15.6	0.27
		−4.21		−2.95		17.61		−4.33
P17^{1}	−7.2	7.84	−28.5	15.48	−11.6	6.06	−12.0	16.30
		5.73		6.82		−2.64		4.75
M18^{1}	−64.8	31.33	−58.0	29.55	3.3	−3.87	−61.7	30.30
C. Assignment of Heme Resonances for c3Db at pH 8.2 and 303 K								
M2^{1}	−48.2	19.96	−31.0	8.23	−32.3	14.15	−28.2	8.88
H3^{1}	n.d.	n.d.	n.d.	n.d.	−29.1	−2.50	n.d.	n.d.
H3^{2}	n.d.	n.d.	n.d.	n.d.	77.7	−3.44	n.d.	n.d.
M7^{1}	−15.7	9.17	−33.5	19.37	−36.6	13.51	−32.9	14.44
H8^{1}	n.d.	n.d.	−32.6*	0.96*	n.d.	n.d.	n.d.	n.d.
H8^{2}	n.d.	n.d.	15.3*	−2.09*	n.d.	n.d.	n.d.	n.d.
M12^{1}	−52.6	19.72	−35.1	11.22	−34.7	20.08	−31.9	8.94
P13^{1}	4.0*	2.13*	−1.0	0.78	n.d.	26.41	−14.7	0.96
		−3.67*		−0.62		19.31		−1.50
P17^{1}	−3.2	6.82	−22.6	10.46	−13.5	3.48	−31.9	13.51
		1.49		9.93		3.19		3.01
M18^{1}	−58.5	27.23	−57.9	27.99	−2.9	−1.03	−44.4	20.02
D. Assignment of Heme Resonances for c3Dn at pH 5.0 and 298 K								
M2^{1}	−50.1	20.73	−30.1	7.36	−32.3	13.93	−29.1	9.00
H3^{1}	n.d.	n.d.	n.d.	n.d.	−29.7	−2.67	n.d.	n.d.
H3^{2}	n.d.	n.d.	n.d.	n.d.	−79.3	−3.60	n.d.	n.d.
M7^{1}	−15.1	8.77	−35.1	20.26	−37.9	13.93	−32.9	14.39
H8^{1}	n.d.	n.d.	−33.5*	0.79*	n.d.	n.d.	n.d.	n.d.
H8^{2}	n.d.	n.d.	15.2*	−2.08*	n.d.	n.d.	n.d.	n.d.
M12^{1}	−48.8	17.44	−35.7	11.29	−33.8	19.44	−31.6	8.47
P13^{1}	5.3	1.08	−1.3	0.44	−68.8	25.36	−14.4	0.50
		−4.14		−1.20		19.85		−1.67
P17^{1}	−5.7	7.53	−23.2	11.64	−14.4	3.37	−33.5	13.63
		2.31		8.59		3.08		3.02
M18^{1}	−59.4	27.88	−58.8	28.41	−2.6	−1.44	−44.7	20.03

[a] The hemes are numbered in the order of their cysteinyl ligands in the cytochrome c_3 amino acid sequences. Asterisks denote tentative assignments.

shifts, and the fits then predict shifts for 3CH and 13CH$_2$ which are close to the average of the observed shifts in each case. The availability of shifts from diametrically opposed ^{13}C nuclei allows such distortions to be averaged out and is, therefore, a significant advantage.

To ensure that the results obtained for all the hemes are comparable, the hyperfine coupling constant,[21] Q_{cc}, was fixed at −36 MHz while the molecular orbital coefficients, used in common for all hemes, were optimized. Only two of these parameters are independent; suitable choices are either c_1 and c_5 or Q_{cc} and the ratio c_1/c_5. Previously, Q_{cc} has been treated as a variable while c_1 and c_5 were both fixed at values obtained from simple Hückel calculations,[26] but the number of hemes studied in this work provides the opportunity to determine new empirical values for the coefficients. The orientation of the rhombic perturbation, θ, and the energy splitting of the orbitals, ΔE, obtained from the fit of the ^{13}C paramagnetic shifts of each heme, excluding all tentative assignments, are reported in Table 3. The results of fitting data previously reported for c3D[32] are also included.

The maximum error which might be introduced by the neglect of intrinsic dipolar shifts was assessed by model calculations with a magnetic susceptibility tensor typical of parallel ligands, which generate the largest possible equatorial anisotropy (set at $\Delta\chi_{eq} = -1.5 \times 10^{-32}$ m^3), and the assumption of counter-rotation of the magnetic axes with respect to a rhombic perturbation normal to the ligand planes.[27] Aligning the imidazole planes with heme *meso* protons enhances the anisotropy

Table 2. Assignment of ^{13}C Resonances for Nuclei Positioned α to the Heme

	c3Dg pH 6.3 $T = 307$ K	c3Dg pH 9.4 $T = 298$ K	c3Dg pH 9.4 $T = 307$ K	c3Dd pH 7.4 $T = 307$ K	c3Dn pH 5.0 $T = 308$ K	c3Db pH 8.2 $T = 293$ K
			heme 1			
M2^1	−38.3	−40.4	−38.2	−48.6	−47.6	−50.7
H3^1	n.d.	n.d.	n.d.	n.d.	n.d.	n.d.
M7^1	−16.3	−17.5	−16.0	−5.6	−14.1	−16.6
H8^1	−39.0	−42.4	−38.9	−33.9	n.d.	n.d.
M12^1	−45.8	−48.0	−45.4	−54.7	−46.6	−55.1
P13^1	11.2	11.2	11.0	7.5	n.d.	4.0*
P17^1	−7.1	−8.3	−6.6	−3.5	−4.8	−4.1
M18^1	−62.2	−65.4	−61.8	−58.2	−56.9	−61.6
			heme 2			
M2^1	−23.7	−24.7	−23.2	n.d.	−28.8	−32.3
H3^1	17.4*	15.9*	17.7*	n.d.	n.d.	n.d.
M7^1	−35.8	−38.1	−35.4	−40.5	−32.9	−35.4
H8^1	−32.0	−35.0	−31.4	−27.8	−31.0*	−35.4*
M12^1	−26.7	−27.8	−26.4	−22.3	−34.4	−36.3
P13^1	4.0	3.7	4.4	−11.3	n.d.	−1.6
P17^1	−26.4	−28.6	−25.9	−22.3*	−21.3	−24.1
M18^1	−55.0	−57.5	−54.7	−46.9	−56.0	−61.0
			heme 3			
M2^1	−32.2	−34.3	−31.7	−32.9	−30.1	−34.1
H3^1	−29.4	−31.8	−29.2	−27.8	−27.3	−31.6
M7^1	−27.0	−28.8	−26.8	−27.4	−36.3	−38.2
H8^1	n.d.	n.d.	n.d.	n.d.	n.d.	n.d.
M12^1	−37.3	−39.4	−36.9	−40.1	−31.9	−36.6
P13^1	−51.6	−54.8	−51.1	−57.8	−64.8	n.d.
P17^1	−10.1	−11.7	−10.0	n.d.	−12.9	−14.5
M18^1	3.4	3.3	3.3	−0.1	−2.6	−2.9
			heme 4			
M2^1	−42.4	−44.8	−42.0	−46.5	−27.6	−29.7
H3^1	22.3*	22.2*	21.7*	n.d.	n.d.	n.d.
M7^1	−11.4	−12.1	−11.1	−6.9	−31.3	−34.7
H8^1	−34.9*	−36.0*	−32.1*	−32.8	n.d.	n.d.
M12^1	38.0	−40.1	−37.6	−44.5	−30.4	−33.2
P13^1	15.0*	15.6	15.7*	11.2	−12.9	−16.0
P17^1	n.d.	−12.1	−11.3	−3.4*	−31.3	−34.8
M18^1	−59.0	−61.6	−58.4	−56.5	−42.6	−46.6

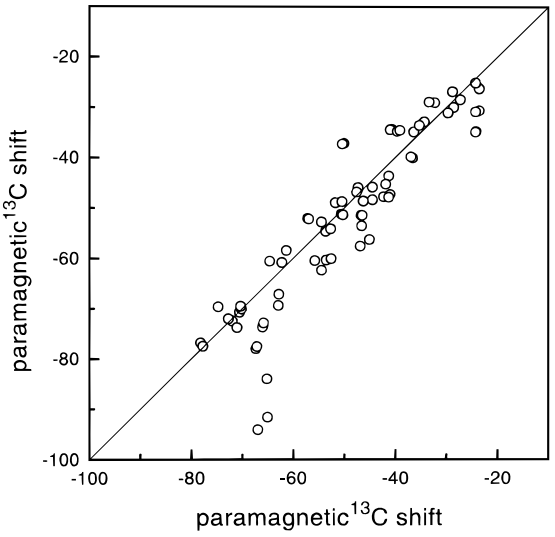

Figure 1. Paramagnetic ^{13}C shifts for heme α substituents, each plotted against the shift of the diametrically opposed substituent (substituents 2, 3, 7, 8 on the *x*-axis, 12, 13, 17, 18 on the *y*-axis). The line is drawn for guidance with unit slope, passing through the origin.

of the paramagnetic shifts and increases the apparent ΔE value by up to 0.5 kJ mol^{-1}, whereas alignment with pyrrole nitrogens may reduce the value by up to 1.0 kJ mol^{-1}. The error introduced in θ is zero in these orientations, with a maximum deviation of 4° found at intermediate positions.

The orientation of the bisector of the normals of the histidine planes, ϕ, and the acute angle between the axial histidines, β, was obtained for each heme from X-ray structures and are reported in Table 4.[40−44] The values of θ obtained from the model are plotted against the values of ϕ from crystal structures in Figure 2 and show an excellent correlation. Although the precision of the X-ray structures can be assumed to be high, part of the difference between values of θ and ϕ may be attributed to differences between the structures in solution and in the crystal. The differences between the two molecules of c3Dv found in the unit cell also provide some estimate of the possible distortions in the crystalline state, with values of ϕ which vary by up to 8°, which is larger than the maximum possible error induced by neglecting intrinsic dipolar shifts.

The values calculated for the orbital energy splitting parameter, ΔE, are plotted against the acute angle between the planes of the axial histidines, β, in Figure 3. This shows a clear relationship that is in broad agreement with the expression $\Delta E = 5 \cos \beta$ kJ mol^{-1} proposed previously.[22] The most striking

(40) Czjzek, M.; Payan, F.; Guerlesquin, F.; Bruschi, M.; Haser, R. *J. Mol. Biol.* **1994**, *243*, 653−667.
(41) Morais, J.; Palma, P. N.; Frazão, C.; Caldeira, J.; LeGall, J.; Moura, I.; Moura, J. J. G.; Carrondo, M. A. *Biochemistry* **1995**, *34*, 12830−12841.
(42) Matias, P. M.; Morais, J.; Coelho, R.; Carrondo, M. A.; Wilson, K.; Dauter, Z.; Sieker, L. *Protein Sci.* **1996**, *5*, 1342−1354.
(43) Matias, P. M.; Frazão, C.; Morais, J.; Coll, M.; Carrondo, M. A. *J. Mol. Biol.* **1993**, *234*, 680−699.
(44) Coelho, A. V.; Matias, P.; Frazão, C.; Carrondo, M. A. *Fourth European Workshop on Crystallography of Biological Macromolecules*; Como, Italy 1995.

Table 3. Molecular Orbital Parameters Obtained from the Fit of the ^{13}C Chemical Shift of the α Substituents of the Heme[a]

	c3Dg (pH 6.3)		c3Dg (pH 9.4)		c3Dv (pH 5.0)		c3Dv (pH 9.0)		c3Dd (pH 7.4)		c3Db (pH 8.2)		c3Dn (pH 5.0)	
	θ	ΔE	θ	ΔE	θ	ΔE	θ	ΔE	θ	ΔE	θ	ΔE	θ	ΔE
heme **1**	−29.6	4.83	−29.2	4.84	−34.4	4.70	−34.4	4.83	−40.4	4.51	−37.5	3.81	−35.8	3.83
heme **2**	−11.7	4.13	−11.8	4.09	−4.5	2.47	−5.2	2.32	−5.2	2.70	−17.3	3.25	−16.9	3.42
heme **3**	77.1	5.40	77.0	5.31	75.4	5.37	76.7	5.51	76.6	5.42	73.7	5.56	72.9	5.34
heme **4**	−29.9	4.35	−29.0	4.56	−30.1	5.19	−29.3	5.28	−36.8	4.19	−8.1	1.45	−8.2	1.47

[a] A hyperfine coupling constant of −36 MHz was used and values for c_1 (0.137) and c_5 (0.071) were fitted for all hemes simultaneously. The parameters for the hemes of c3Dv were recalculated from assignments reported in the literature.[32] The value of θ is expressed in degrees, and that of ΔE is given in kJ mol^{-1}.

Table 4. Geometry of the Axial Ligands of the Hemes Determined from the X-ray Structures of the Various Cytochromes c_3[40−44,a]

	c3Dg (pH 6.5)		c3Dv (A) (pH 5.5)		c3Dv (B) (pH 5.5)		c3Dd (pH 4.0)		c3Db (pH 8.0)		c3Dn (pH 7.7)	
	ϕ	β	ϕ	β	ϕ	β	ϕ	β	ϕ	β	ϕ	β
heme **1**	−34.6	4.0	−35.5	4.7	−36.7	2.4	−39.2	9.8	−34.8	7.6	−32.7	5.0
heme **2**	−8.6	52.0	−5.8	55.4	3.2	72.1	−2.2	60.2	−13.6	61.9	−19.8	50.0
heme **3**	66.1	13.6	65.1	11.2	69.3	13.6	66.9	5.3	61.8	23.4	58.8	25.6
heme **4**	−31.0	15.0	−36.8	8.2	−36.8	7.4	−42.0	1.4	−6.9	70.8	−1.1	77.2

[a] The angle between the bisector of the acute angle between the normals to the histidine planes and the vector defined by the pyrrole nitrogens C and A of the heme is labeled ϕ, and β is the acute angle between the axial histidines, all expressed in degrees.

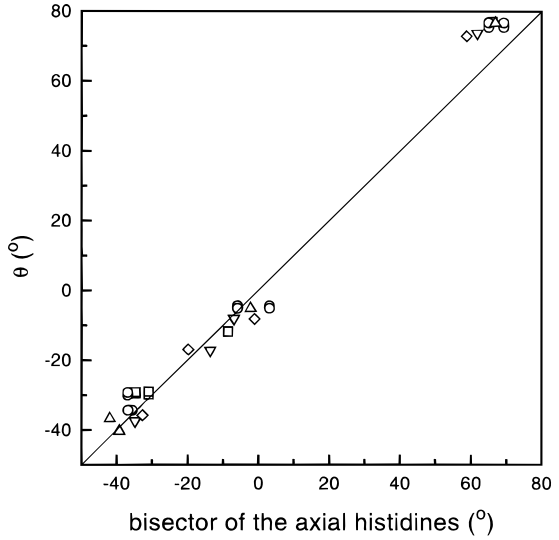

Figure 2. The orbital mixing parameter, θ, versus the orientation of the bisector of the normals to the axial histidine planes taken from the X-ray structures. Both angles are referred to the NC-NA vector.[26] The various cytochromes are represented by (□) c3Dg at two pH values, (○) c3Dv at two pH values with two molecules per unit cell, (△) c3Dd, (▽) c3Db, and (◇) c3Db.

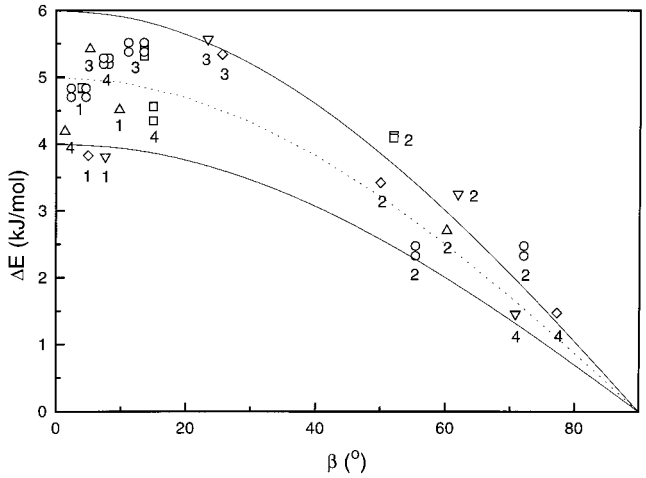

Figure 3. Energy splitting of the molecular orbitals, ΔE, versus the angle between the normals of the axial histidine planes, β, obtained from the X-ray structures. The dotted line represents the empirical expression[22] $\Delta E = 5 \cos \beta$ kJ mol^{-1} and the continuous lines show the maximum and minimum limits determined by $\Delta E = (5 + \cos 4\theta) \cos \beta$ kJ mol^{-1}. The symbols are defined in Figure 2, and Arabic numerals close to the symbols indicate the corresponding heme.

deviations are observed for hemes **2** of c3Dv (molecule A), c3Db, and c3Dg. Once again, part of the scatter may be accounted for by uncertainties in the values of β taken from crystal structures, exemplified by a difference for heme **2** of almost 20° between the two molecules in the unit cell of crystalline c3Dv. The deviations suggest that the geometry of the axial ligands of heme **2** may be less tightly constrained in these molecules, and the geometry observed in at least one of the X-ray structures of c3Dv clearly cannot reflect the situation in solution. Moreover, the NMR data obtained at pH 5.0 and 9.0 for c3Dv and at pH 6.3 and 9.4 for c3Dg show that only small variations are to be expected as a result of pH changes.

However, the uncertainty in β does not explain the scatter for hemes with near-parallel ligands. One possible explanation for the variation in ΔE when β is small lies in the pseudo-Jahn−Teller effect, which was invoked to explain a dependence of V/Δ on ϕ found in low-temperature EPR studies of model compounds.[9,45] We have also explored the dependence of the energy separation of the π molecular orbitals on ϕ by means of extended Hückel calculations. These calculations were performed with the program CACAO[46] with a bis-imidazole porphyrin complex with eight methyl substituents and idealized geometry. The parameters were taken from Hoffman,[47] with the Fe 3d ionization potential adjusted to −11.60 eV to improve agreement with the coefficients found for the frontier molecular orbitals. Although the calculated values must be regarded as qualitative, being approximately four times smaller than the fitted values of ΔE, the cosine dependence of the splitting on β is correctly simulated. The results were unaffected by rotating one imidazole through 180°, reflecting the approximate C_{2v} symmetry of the ligands. Furthermore, the calculation reveals that the maximum splitting, obtained for $\beta = 0$, also depends on cos 4θ, with a range of about 30%.

A plot of ΔE against θ is shown in Figure 4, restricted to those hemes with an angle β smaller than 30° in the crystal

(45) Soltis, S. M.; Strouse, C. E. *J. Am. Chem. Soc.* **1988**, *110*, 2824−2829.
(46) Mealli, C.; Proserpio, M. *J. Chem. Educ.* **1990**, *67*, 399−402.
(47) Hoffman, R. J. *Chem. Phys.* **1963**, *39*, 1397−1412

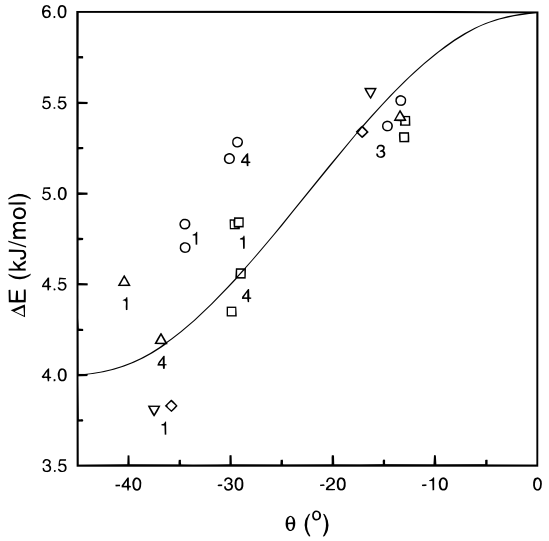

Figure 4. Energy splitting of the molecular orbitals versus the 90° modulus of the orientation of the rhombic perturbation, plotted for hemes with values of β less than 30° in the crystal structures. The line represents the empirical formula $\Delta E = (5 + \cos 4\theta)$ kJ mol^{-1} for parallel axial ligands ($\beta = 0$) to show the angular dependence. The symbols and numbers are defined as in Figures 2 and 3.

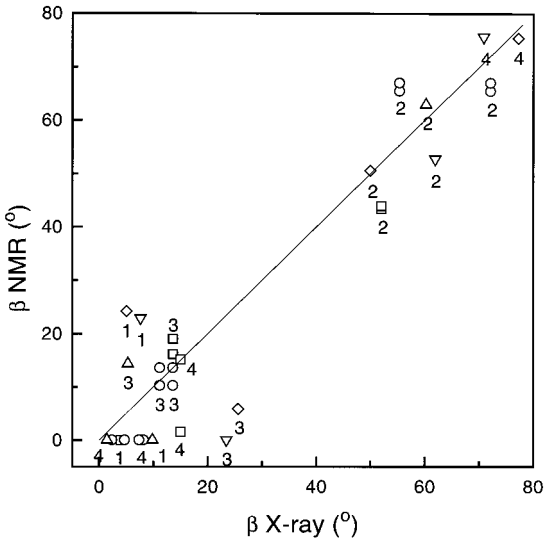

Figure 5. Correlation between β, calculated from ^{13}C NMR by using the empirical formula $\Delta E = (5 + \cos 4\theta) \cos \beta$, and β, measured from X-ray crystal structures. The line is drawn with unit slope passing through the origin. The symbols and numbers are defined as in Figures 2 and 3.

structures which should, therefore, have ΔE values close to a maximum. Despite considerable scatter, this reveals a clear trend in the data, which may be approximated by $\Delta E_{max} = 5 + \cos 4\theta$ kJ mol^{-1}, since the amplitude of the variation is coincidentally close to unity (fitted coefficients 5.04 and 0.78). It is important to note that this trend is conservatively estimated because it is of opposite sign to the small systematic errors generated by neglecting intrinsic dipolar shifts.

The limiting curves obtained with the extreme values of ΔE_{max} are shown in Figure 3. Even neglecting the second-order effect, it is apparent that ΔE may be used to estimate β with a precision similar to that obtained from Karplus curves, which relate vicinal *J*-couplings to dihedral angles.[48] This relationship also appears to be sufficiently accurate to detect differences between the angle β observed in the crystal and that in solution, as may be the case for hemes **2** from c3Dg, c3Db, and c3Dv (molecule A). Alternatively, the computational and empirical evidence, together with the accuracy of θ, would justify using the modified expression $\Delta E = (5 + \cos 4\theta) \cos \beta$ kJ mol^{-1} to calculate values for the angle β from NMR data. The result of applying this expression is shown in Figure 5, where it can be seen that the accuracy increases as β approaches 90° and that the agreement between the calculated values of β and those taken from the crystal structures is comparable with variations among the crystal structures themselves, as represented by the two molecules in the unit cell of c3Dv.

Conclusions

The correlation between the parameters obtained by fitting NMR data and axial ligand orientations in the X-ray structures of the various cytochromes indicates that, even for structures of moderately high resolution, the structure in the crystal may not accurately describe that of the protein in solution. This is exemplified by the considerable differences between molecules A and B of c3Dv, and between c3Dn and c3Db. The amino acid sequences of c3Dn and c3Db differ by only two residues, which are well-separated from the hemes, **2** and **4**, that show the largest difference in geometry. Most importantly, the differences discussed here are not confined to the protein surface but extend into the heme core.

Despite the implicit uncertainty about the structures in solution, this work shows that the orientation of the rhombic perturbation and the energy splitting of the molecular orbitals of the heme are dominated by the orientation of the axial ligands. The large number of examples studied allowed the observation of a cosine dependence of the maximum energy splitting of the orbitals on the ligand orientation, θ, as well as on the dihedral angle, β. This higher order correction allows the orientation of the axial ligands in solution to be determined directly from NMR data with similar confidence to that expected from X-ray diffraction, even when the dipolar contributions to the paramagnetic shifts are neglected. Since this analysis uses the assignment only of resonances from the heme substituents, knowledge of the structure of the surrounding protein is not required, but the information is ambiguous insofar as the two ligands (proximal and distal) are not distinguished, nor is the C2 and C4 edge of each imidazole. However, this method gives a confidence limit of about ±10° for each ligand plane, and this should be sufficient in most cases to assign orientations to specific ligands on the basis of preliminary solution structures. It is usually impossible to observe NOE effects involving the imidazole protons of histidinyl residues ligated to ferrihemes, and the critical region of the heme pocket cannot be well-defined by distance constraints alone. Orientational constraints based on HMQC data may, therefore, be essential to obtaining accurate structures for paramagnetic heme proteins in solution.

An analogous use of complementary structural information derived from paramagnetic shifts has been demonstrated for the methylene protons and α-carbon of cysteinyl ligands in $[Fe_4S_4]^{2+}$ clusters.[49] That is a more straightforward case insofar as the measurement involves nuclei of the rotatable group directly and is a function of a single torsion angle. The extensive experimental database reported here for bis-histidinyl hemes should allow reasonably tight restraints on the ligand orientations to be used with confidence, and their influence on the structure is enhanced by propagation through the rigid imidazole rings.

(48) Karplus, M. *J. Chem. Phys.* **1959**, *30*, 11−15.

(49) Bertini, I.; Capozzi, F.; Luchinat, C.; Piccioli, M.; Vila, A. J. *J. Am. Chem. Soc.* **1994**, *116*, 651−660.

In addition, by assuming that the major magnetic axis is perpendicular to the heme plane, the counter-rotation of the rhombic perturbation and the principal axes of the magnetic susceptibility tensor allows the orientation of the axes to be determined within a few degrees.[28] This is a useful aid in the early stages of assigning spectra and structure determination of paramagnetic heme proteins. The approximate orientation of the magnetic axes may also be used to constrain the tensor when calculating complete protein structures with the inclusion of dipolar shifts.[17]

Finally, it should be noted that the trends found in the energy separation of the heme molecular orbitals as a function of ligand orientation are similar to those observed by EPR and analyzed in terms of iron atomic orbitals.[6,9,50] The influence of the resultant orientation of the two ligands, θ, has been attributed to a pseudo-Jahn−Teller distortion, with the supporting evidence of a slight anisotropy in the iron−porhyrin nitrogen bond lengths found in cationic complexes. We find that the angular dependence of orbital overlap would account for this effect without the need for geometric distortion, and this seems to be a more probable explanation, at least in solutions of heme proteins, in which the symmetry of the macrocycle is generally low.

Acknowledgment. The authors are grateful to Professor J. LeGall for kindly providing the protein samples. This work was supported by PRAXIS XXI (BD 2509/93), PRAXIS/PCN/BIO/0074/96, and EC contract No. ERBFMRXCT980218.

JA983102M

(50) Scheidt, W. R.; Chipman, D. M. *J. Am. Chem. Soc.* **1986**, *108*, 1163−1167.